Optical functionalities of dielectric material deposits obtained from a Lambertian evaporation source

J. M. González-Leal

Department of Condensed Matter Physics. Faculty of Sciences. University of Cadiz. 11510 – Puerto Real (Cadiz). Andalusia. Spain
juanmaria.gonzalez@uca.es

http://www.uca.es/dpto/C143

Abstract: The thickness profile of deposits obtained from Lambertian evaporation sources is highlighted concerning its transmission optical functionality, in the case of dielectric materials. Fresnel diffraction is used to characterize the lateral resolution and intensity on the optical axis of an input gaussian laser beam. Functionality similar to logarithmic axicons, with uniform lateral resolution and also uniform on-axis intensity, is theoretically derived. It is also shown for this particular optical structure that the intensity slope along the optical axis can be changed from positive to negative values by only changing the input beam width.

OCIS codes: (220.1250) Aspherics; (310.1860) Deposition and fabrication

References and links

1. R. Glang, in: *Handbook of Thin Film Technology* L.I. Maissel and R. Glang eds., (McGraw-Hill, New York, 1983).
2. M. Born, E. Wolf, Principles *of optics: Electromagnetic theory of propagation, interference and diffraction of light* 6th ed. (Pergamon Press, Oxford, 1989) p. 752.
3. J. M. González-Leal, R. Prieto-Alcón, J. A. Ángel, D. A. Minkov, E. Márquez, "Influence of the substrate absorption on the optical and geometrical characterization of thin dielectric films," Appl. Opt. **41**, 7300 (2002).
4. A. T. Friberg, "Stationary-phase analysis of generalized axicons," J. Opt. Soc. Am. A **13**, 743 (1996).
5. J. H. McLeod, "The axicon: A new type of optical element," J. Opt. Soc. Am. **44**, 592 (1954).
6. A. Burvall, K. Kolacz, Z. Jaroszewicz, A. T. Friberg, "Simple lens axicon," Appl. Opt. **43**, 4838 (2004).
7. Z. Jaroszewicz, A. Burvall, A. T. Friberg, "Axicon: the most important optical element," Opt. Photon. News **16**, 34 (2005).
8. B. P. S. Ahluwalia, W. C. Cheong, X.-C. Yuan, L.-S. Zhang, S.-H. Tao, J. Bu, H. Wang, "Design and fabrication of a double-axicon for generation of tailored self-imaged three-dimensional intensity voids," Opt. Lett. **31**, 987 (2006).
9. J. X. Pu, H. H. Zhang, and S. Nemoto, "Lens axicons illuminated by Gaussian beams for generation of uniform-axial intensity Bessel fields," Opt. Eng. **39**, 803 (2000).
10. J. Sochacki, A. Kolodziejczyk, Z. Jaroszewicz, and S. Bará, "Nonparaxial designing of generalized axicons," Appl. Opt. **31**, 5326 (1992).
11. R. Grunwald, U. Neumann, A. Rosenfeld, J. Li, P. R. Herman, "Scalable multichannel micromachining with pseudo-nondiffracting vacuum ultraviolet beam arrays generated by thin-film axicons," Opt. Lett. **31**, 1666 (2006).
12. J. W. Goodman, *Introduction to Fourier optics* (McGraw-Hill, Singapore, 1996).
13. H. Kogelnik,"Coupled-wave theory for thick hologram gratings," Bell Syst. Tech. J. **48**, 2909 (1969).

1. Introduction

Effusion is a well-known process in physical vapour deposition [1], in which individual molecules at thermal equilibrium flow through a hole, without collisions. This phenomenon manifests in a matter irradiance (i.e., mass per unit of evaporating area and unit of time) being

#79571 - $15.00 USD Received 6 Feb 2007; revised 27 Feb 2007; accepted 24 Mar 2007; published 20 Apr 2007

proportional to the cosine of the angle between the observer's sight and the evaporation surface normal, in similar fashion to the optical phenomenon observed in Lambertian surfaces, whose light irradiance also follows the same angular dependence [2]. As a consequence of the cosine law, the radiance of matter or light, from a Lambertian evaporation source or a Lambertian reflectance surface, respectively, measured by the observer at any view angle around the source or surface, is constant, as the area saw by the observer also depends on the cosine of the view angle.

Differently to the Lagmuir isotropic free-evaporation sources, Lambertian sources provide a material distribution following the above-introduced Lambert cosine law [1,2]. This fact is widely used for the uniform deposition of films onto inner spherical surfaces. Evidently, the same fact makes the deposits non-uniform in thickness when collected onto flat substrates, and it is a well-known drawback for planar technologies. Conventional approaches to reduce thickness inhomogeneities in the thin-film deposits involve substrates rotating around an axis far from the evaporation axis, and large substrate-source distances [1,3]. Nonetheless, the thickness profile of deposits condensed onto transparent substrates placed close to the evaporation source, will be shown here to have technological interest.

The paper is organized as follows: A brief overview on the physics behind the effusion process is made at the next section, with the aim to eventually introduce the thickness profile of the deposits when collected onto flat substrates. Assuming we are dealing with dielectric materials, the amplitude transmission function for the deposits is derived, and the intensity field behind this particular refractive optical structure for laser incidence, is studied on the basis of the stationary-phase approximation for the Fresnel diffraction integral [2,4]. The results show an optical functionality for these refractive structures similar to that observed in axicons, concerning focal depth, lateral resolution and intensity slopes [5-11]. The dependence of these optical parameters on the design parameters for these particular refractive optical structures is discussed. Finally, the most relevant results are summarized in the concluding remarks, and they are highlighted against some established techniques for axicon fabrication.

2. Theory

2.1 Lambertian evaporation: cosine law

The effusion evaporation regime can be achieved using a Knudsen cell [1]. This device consists in a crucible jailed into a box having a small aperture on top. The device guarantees multiple reflections of the evaporated molecules at the inner-box sides, in such a fashion that thermalization, and in turn, maxwellian-boltzmann distribution for velocities is achieved inside the box. The small size of the cell aperture assures no molecules come back into the evaporation source, which makes the so-called sticking parameter $\sigma_v = 1$ in Hertz-Knudsen equation [1]. This results in the following mathematical relation for the evaporated mass about an exit angle of θ into the forward solid angle $d\omega$

$$dM_e = M_e \cos(\theta)\frac{d\omega}{\pi}: \qquad (1)$$

this cosine dependence for the mass emission being similar to that observed in the photon emission from Lambertian surfaces.

If eventually, a flat substrate is placed in the evaporation chamber as illustrated in Fig. 1, the mass of condensed material per unit area on the substrate surface can be derived from Eq. (1)

$$\frac{dM_c}{dA_c} = \frac{M_e}{\pi\rho^2}\cos(\theta)\cos(\psi), \qquad (2)$$

on the basis of both mass conservation law, $dM_c = dM_e$, and the projection of the elemental area $\rho^2 d\omega$ onto the substrate at an angle of Ψ (see Fig. 1).

#79571 - $15.00 USD Received 6 Feb 2007; revised 27 Feb 2007; accepted 24 Mar 2007; published 20 Apr 2007

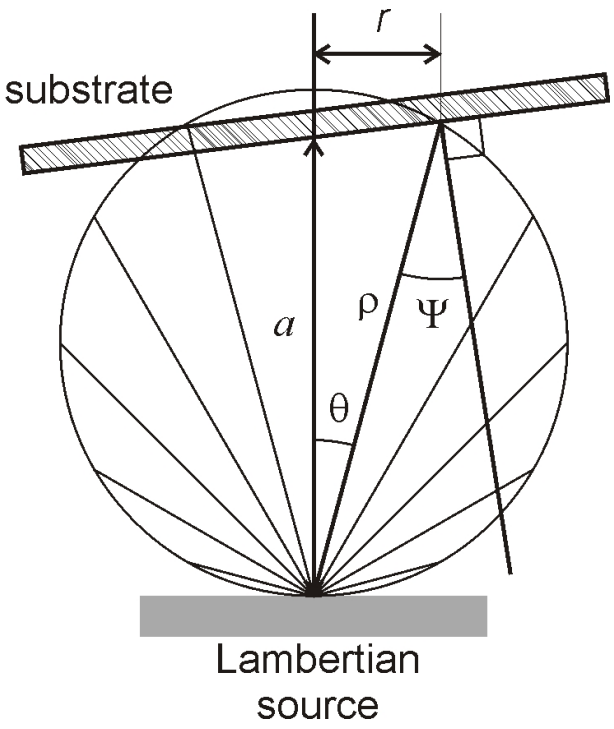

Fig. 1. Illustration of the cosine law for the evaporated-mass distribution from Lambertian evaporation source. A flat substrate is also drawn and relevant deposition parameters are indicated: *a* being the distance from the centre of the source to the substrate, ρ the modulus of the vector from the centre of the source to any point on the substrate surface, θ is the angle between *a* and ρ, and Ψ is the angle between ρ and the normal vector to the surface substrate.

In the case of a substrate facing parallel to the cell aperture $\Psi = 0$, and the thickness profile of the deposit can be easily derived from the sketch illustrated in Fig. 1. In this case $\cos(\Psi) = \cos(\theta) = a/\rho = a/(a^2 + r^2)^{1/2}$, and Eq. (2) can be written as

$$\frac{dM_c}{dA_c} = \frac{M_e}{\pi} \frac{a^2}{(a^2 + r^2)^2}. \tag{3}$$

As surface density scales thickness if volume density is constant, which is the case for deposits with homogeneous composition, the thickness profile of the deposited material will follow the same dependence on *r* as given in Eq. (3),

$$t(r) = \frac{A}{(1+(r/a)^2)^2}, \tag{4}$$

with *A* standing for the maximum thickness of deposited material at $r = 0$. For illustrative purposes a plot of Eq. (4) for $A = 1$ μm and $a = 1$ mm, is shown in Fig. 2.

2.2 Optical function analysis

If the deposit is made with a dielectric material with refractive index *n*, the amplitude transmission function of such a refractive optical structure would be, from Eq. (4) [2,4,12]

$$\varphi(r) = A(n-1)(1-t(r)) = A(n-1)\left(1 - \frac{1}{(1+(r/a)^2)^2}\right). \tag{5}$$

The light field at polar coordinates *r'* and *z* on the image plane behind this refractive optical structure, can be analysed by solving Fresnel diffraction integral [2,4,12]

#79571 - $15.00 USD Received 6 Feb 2007; revised 27 Feb 2007; accepted 24 Mar 2007; published 20 Apr 2007

$$U(\rho,z)=\frac{e^{ikz}}{i\lambda z}e^{i\frac{k}{2z}\rho^2}\int_S U(r,z)e^{i\frac{k}{2z}r^2}e^{-i\frac{k}{z}r\rho\cos(\phi)}\,d\phi\,dr\ . \tag{6}$$

Integration in Eq. (6) is performed over polar coordinates r and ϕ at the object plane, into the surface S. $U(r, z)$ is the incident light field, λ the wavelength, and $k = 2\pi/\lambda$. $U(r, z)$ can be determined from the amplitude transmission function $\varphi(r)$ of Eq. (3). If gaussian intensity distribution with width σ at I_0/e^2 is further considered for the input light, $U(r, z)$ can be eventually written as

$$U(r,z)=U(r)=e^{-(r/\sigma)^2}\,e^{-ik\varphi(r)}\ . \tag{7}$$

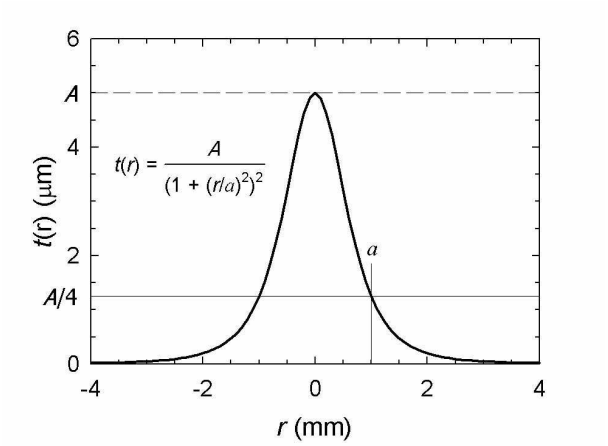

Fig. 2. Thickness profile, $t(r)$, corresponding to a deposit obtained from a Lambertian evaporation source. The analytical formula for $t(r)$ and design parameters A and a are conveniently indicated.

On the other hand, as we are dealing with thickness profiles with circular symmetry, the integral over the angle ϕ can be shown to give the Bessel function of first kind and zero order [12], and Eq. (7) can eventually be written as follows:

$$U(\rho,z)=\frac{e^{ikz}}{ikz}e^{i\frac{k}{2z}\rho^2}\int_S e^{-(r/\sigma)^2}\,e^{ik\left(\frac{r^2}{2z}-\varphi(r)\right)}J_0\left(\frac{k\rho r}{2z}\right)r\,dr=$$

$$=\frac{e^{ikz}}{ikz}e^{i\frac{k}{2z}\rho^2}\int_S e^{-(r/\sigma)^2}\,e^{ikf(r)}J_0\left(\frac{k\rho r}{2z}\right)r\,dr\,, \tag{8}$$

where $f(r) = r^2/(2z) - \varphi(r)$.

In the case of the amplitude transmission function given by Eq. (3), the integral of Eq. (8) can be solved by the stationary-phase approximation [2, 4] with critical point

$$r_c=a\left(\left(\frac{4A(n-1)z}{a^2}\right)^{1/3}-1\right)^{1/2} \tag{9}$$

fulfilling the equation $\left.\frac{df}{dr}\right|_{r_c}=0$. The solution for the intensity in the case of fully coherent illumination being, finally

#79571 - $15.00 USD Received 6 Feb 2007; revised 27 Feb 2007; accepted 24 Mar 2007; published 20 Apr 2007

$$I(r',z) \propto e^{-2(r_c/\sigma)^2} \frac{r_c^2}{z^2} \frac{1}{1/z + \varphi''(r_c)} J_0^2\left(\frac{k\, r_c\, r'}{2z}\right). \tag{10}$$

2.3.1 Lateral resolution

The width of the light beam, *w*, behind the refractive optical structure under study, can be found solving equation

$$J_0^2\left(\frac{k\, r_c\, w}{4z}\right) = \frac{1}{2}, \tag{11}$$

where the full width at half maximum (FWHM) is assumed to characterize the lateral resolution. Plot of $w(z)$ for a gaussian incident laser beam with σ = 2 mm, and values for the design parameters A = 5 μm, a = 1 mm and n = 2 , is shown in Fig. 3.

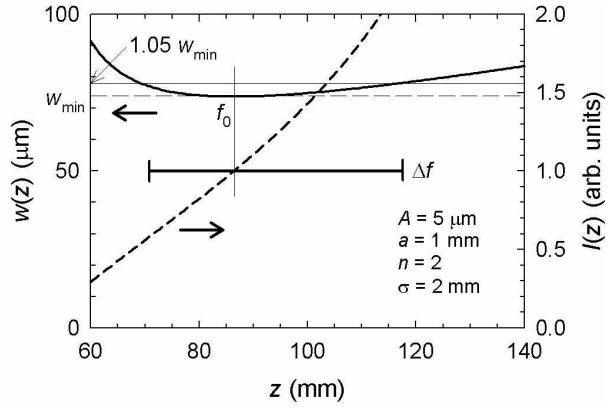

Fig. 3. Lateral resolution (thick solid line) and light intensity (thick dashed line) along the axis for a representative refractive optical structure with design and input gaussian-beam parameters shown in the figure. Thin dashed line indicates the minimum lateral resolution, w_{min}, reached at distance f_0, and thin solid line at a value of the resolution 5 % above w_{min}, is also plotted to characterize the focal region Δf as described in the text (f_0 = 86 mm, w_{min} = 74 μm, and $\Delta f \approx$ 43 mm).

A minimum lateral resolution, w_{min}, is observed in Fig. 3, which appears at distance of f_0 from the refractive optical structure. This distance can be determined from the design parameters a, A and n, solving the equation

$$\left.\frac{d}{dz}\left(J_0^2\left(\frac{k\, r_c\, w}{4z}\right)\right)\right|_{f_0} = \left.\frac{d}{dz}\left(\frac{r_c}{z}\right)\right|_{f_0} = 0, \tag{12}$$

and it can be checked to be given by

$$f_0 = \frac{54}{125} \frac{a^2}{A(n-1)}. \tag{13}$$

Finally, w_{min} can be derived numerically by solving Eq. (12) at f_0, and it can be probed to give the following approximated relationship

$$w_{min} = w(f_0) \approx 1.13 \frac{216a}{25\sqrt{5}\, k\, A(n-1)}. \tag{14}$$

#79571 - $15.00 USD Received 6 Feb 2007; revised 27 Feb 2007; accepted 24 Mar 2007; published 20 Apr 2007

2.3.2 Focal-region intensity

Under the assumptions of the stationary-phase approximation, the intensity will be modulated along the axis as

$$I(0,z) \propto e^{-2(r_c/\sigma)^2} \frac{r_c^2}{z^2} \frac{1}{1/z + \varphi''(r_c)}, \tag{15}$$

where $\varphi''(r_c) = \left. \frac{d^2\varphi(r)}{dr^2} \right|_{r_c}$. The plot of the on-axis intensity normalized to the intensity value at distance f_0, $I(0, z)/I(0,f_0)$, for a gaussian incident laser beam with σ = 2 mm, and values for the design parameters A = 5 μm, a = 1 mm and n = 2, is shown in Fig. 3.

Finally, it is worth to calculate the first derivative of $I(0, z)$ with respect z, at f_0, from Eq. (15), which is given by

$$\left. \frac{dI(0,z)}{dz} \right|_{f_0} \propto \frac{A^2 (n-1)^2 e^{-\frac{2}{5}(a/\sigma)^2}}{\sigma^2} (10\sigma^2 - 3a^2). \tag{16}$$

Equation (16) allows the minimum for $w(z)$ and the minimum for $I(0, z)$ can be made concurrent at f_0, in similar fashion as logarithmic axicons [10], through the following relationship:

$$\sigma_0 = \left(\frac{3}{10} \right)^{1/2} a. \tag{17}$$

3. Discussion

3.1 Design parameters

Figure 3 illustrates the typical lateral resolution along the optical axis, of a dielectric deposit with thickness profile as given by Eq. (2). A significant depth of focus is observed in the plot, provided certain tolerance is allowed for this parameter around the minimum established by Eq. (14). If tolerance of 5 % is agreed, a depth of focus (or focal region), Δf, of about 40 mm would be attained for the refractive optical structure whose results are shown in Fig. 3.

In order to analyze the effects of the design parameters, plots of $w(z)$ and $I(0, z)/I(0, f_0)$ for two different values of the parameter A are shown in Figs. 4(a) and 4(b). As expected according to Eq. (14), the beam width decreases at the focal region with increasing the A value, and concurrently, the focal region makes shorter. This result is consistent with the typical behaviour observed in lenses when increasing the lens curvature, where the Airy spot makes smaller when increasing the numerical aperture, and depth of focus similarly makes shorter [2]. Also in consistence with the well-known behaviour occurring in spherical lenses, the increase of the refractive-index value leads to a higher lateral resolution, as observed in Figs. 4(c) and 4(d). In all cases illustrated in Figs. 3 and 4, a positive slope is observed in the intensity along z, within the focal region.

Contrarily to the above described cases, the increase of the value of the design parameter a, which is related with the lateral size of the deposit (see Fig. 2), and in turn with the substrate-source distance (see Fig. 1), leads to larger values for $w(z)$ at the focal region, as observed in Fig. 5, and in turn, it increases the focal region. This figure also illustrates the change in the intensity slope from positive to negative values when increasing the value for the a parameter up to a value of 4 mm, for an incident gaussian laser beam with σ = 2 mm. This fact was advanced in the previous section when the coincidence between the minimum for $w(z)$ and $I(0, z)$ was analyzed, and Eq. (17) was introduced.

#79571 - $15.00 USD Received 6 Feb 2007; revised 27 Feb 2007; accepted 24 Mar 2007; published 20 Apr 2007

3.2 Intensity control

Equation (17) can be used as a useful way to control the optical function of a given refractive optical structure obtained from a Lambertian evaporation source. As pointed by Eq. (17), values of σ above and below σ_0, change the slope of the intensity within the focal region from positive to negative, respectively, with no influence on the lateral resolution and focal region location. Such effect has also been reported for axicons and lens axicons fabricated by different means [8, 9]. Plots of the $w(z)$ and $I(0, z)/I(0, f_0)$ for fixed values of the design parameters a, A and n, and values of σ at and around σ_0 are shown in Fig. 6. From a technological point of view, such a kind of actuation on the input laser beam allows getting control on the intensity slope over the focal region. This result provides extra functionalities to the refractive optical structure.

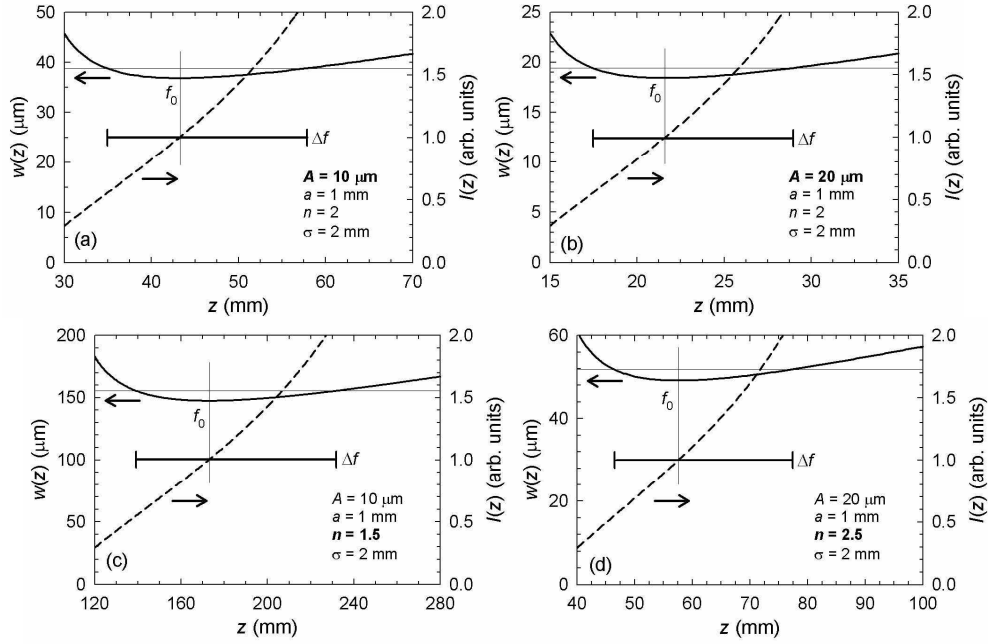

Fig. 4. Lateral resolution (thick solid line) and light intensity (thick dashed line) along the axis for a refractive optical structure with design and input gaussian-beam parameters shown in the figure. Values for f_0 , w_{min}, and Δf are, respectively, 43 mm, 37 μm and 20 mm (a), 22 mm, 18.5 μm and 10 mm (b), 173 mm, 148 μm and 85 mm (c), and 58 mm, 49 μm and 28 mm (d).

#79571 - $15.00 USD Received 6 Feb 2007; revised 27 Feb 2007; accepted 24 Mar 2007; published 20 Apr 2007

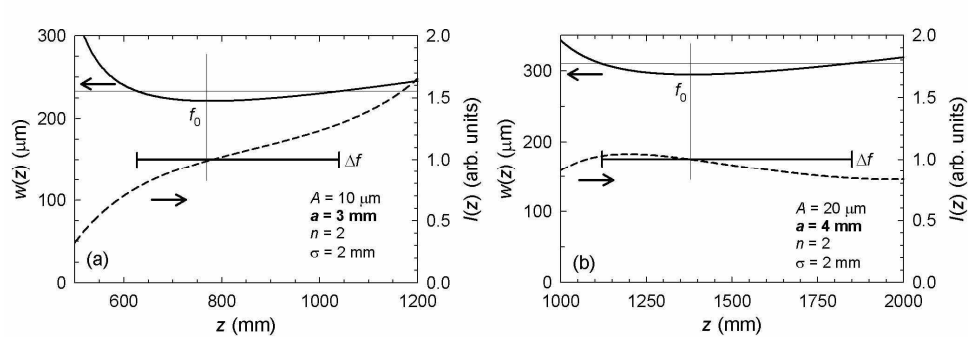

Fig. 5. Lateral resolution (thick solid line) and light intensity (thick dashed line) along the axis for a refractive optical structure with design and input gaussian-beam parameters shown in the figure. Values for f_0 , w_{min}, and Δf are, respectively, 777 mm, 222 μm and 400 mm (a), and 1382 mm, 296 μm and 680 mm (b).

Finally, as typically the gaussian laser beam width is fixed for a laser source, Eqs. (13), (14) and (17) can be used in similar way as design rules to match the specifications of this kind of refractive optical structure to a given working laser beam. For example, for a 532 nm wavelength gaussian laser beam with half-width at $1/e^2$ of σ = 2 mm (Coherent, Verdi V6), a refractive optical structure as those introduced here with focal region around 50 mm and *uniform* intensity, could be fabricated setting the design parameter with values a = 3.65 mm, A = 0.115 mm and n = 2. In this case, a minimum lateral resolution $w_{min} \approx 12$ μm, and a depth of focus $\Delta f \approx 37$ mm, according to the 5 % of tolerance agreed above, can be achieved.

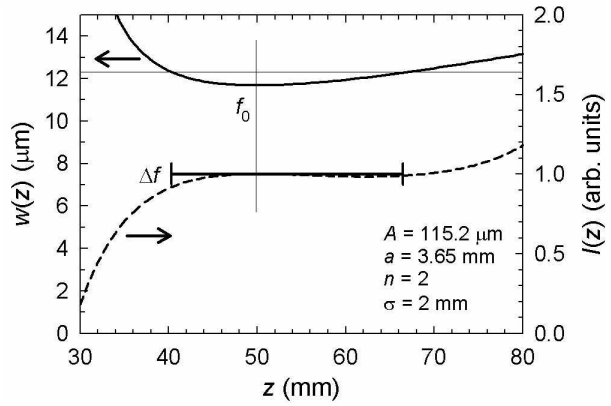

Fig. 6. Lateral resolution (thick solid line) and light intensity (thick dashed line) along the axis for a refractive optical structure with design and input gaussian-beam parameters shown in the figure. Values for f_0 , w_{min}, and Δf are, respectively, 50 mm, 12 μm and 37 mm.

4. Concluding remarks

Axicons and lens axicons, which show *non-diffracting* optical performance, are currently supporting both emerging research fields and technologies dealing with the fundamentals of the light nature, and confocal imaging and optical trapping, as their most remarkable fashions [5-11]. Differently to conventional milling and polishing techniques for optics fabrication, and also differently to expensive lithographic techniques imported from microelectronic technology [8], the present paper probes theoretically the fabrication of these optical devices

#79571 - $15.00 USD Received 6 Feb 2007; revised 27 Feb 2007; accepted 24 Mar 2007; published 20 Apr 2007

in straightforward way from a Lambertian evaporation source, such as a Knudsen cell. In this comparison, it is also worth mentioning that holographic diffractive axicons suffer of the attenuation of the light along thickness sample during the recording, which is a drawback to exploit volume holography characteristics conveniently [13], and approaches for the manufacturing of refractive axicons from thin-film deposition techniques, proposed so far, are complex and involve moving parts [10,11]. The theory introduced here shows practical uniform lateral resolution along the optical axis, with focal depth related to the design parameters *A*, *n* and *a*. Intensity distribution at the focal region has been probed to be dependent on both the design parameter *a* and input laser beam characteristics. In particular, it has been shown that changes in the input beam width, σ, lead to changes in the intensity slope with respect *z* coordinate, from positive to negative values when increasing σ, at given *a*.

Acknowledgments

This work has been partly supported by the Spanish Ministry of Education and Science through the National Physics I+D+i Programme (Spain), under the FIS2005-01409 project, and by the Regional Ministry of Innovation, Science and Enterprise of Andalusia, through the Excellence Research Programme, under the FQM-0654 project. The author wants to thank the anonymous referee for her/his very valuable comments

#79571 - $15.00 USD Received 6 Feb 2007; revised 27 Feb 2007; accepted 24 Mar 2007; published 20 Apr 2007